JOC The Journal of Organic Chemistry

Article

Synthesis of Nonaromatic and Aromatic Dithia Benzisapphyrins

Rima Sengupta, Kishor Gulab Thorat, and Mangalampalli Ravikanth

J. Org. Chem., **Just Accepted Manuscript** • DOI: 10.1021/acs.joc.8b01737 • Publication Date (Web): 07 Sep 2018

Just Accepted

ACS Publications

is published by the American Chemical Society. 1155 Sixteenth Street N.W., Washington, DC 20036

Synthesis of Nonaromatic and Aromatic Dithia Benzisapphyrins

Rima Sengupta,[†] Kishor G. Thorat[†] and Mangalampalli Ravikanth*

Indian Institute of Technology, Powai, Mumbai, 400076, India, Fax:91-22-5723480;

Tel: 91-22-5767176; E-mail: ravikanth@chem.iitb.ac.in

Abstract

A series of [24π] dithia *meta*-benzisapphyrins and [22π] dithia *para*-benzisapphyrins were synthesized by 3+2 condensation of appropriate benzitripyrrane with bithiophene diol under mild acid catalyzed conditions. The dithia *m*-benzisapphyrins and dithia *p*-benzisapphyrins were thoroughly characterized by HR-MS, 1D, 2D NMR, absorption and electrochemical techniques. Our studies showed that dithia *m*-benzisapphyrins are nonaromatic whereas the dithia *p*-benzisapphyrins are aromatic in nature. Thus, we demonstrated here that the dithiabenzisapphyrins can be made aromatic by replacing *m*-phenylene moiety of the benzisapphyrin macrocycle with *p*-phenylene unit. Furthermore, the studies also indicated that the aromaticity of the dithia *p*-benzisapphyrins was relatively more compared to the reported heterosapphyrins. The structural and spectral characteristics including aromaticity of the *m*-benzisapphyrins and *p*-benzisapphyrins were also discussed with the help of DFT, NICS and TD-DFT studies.

Introduction

Sapphyrins **1** (Chart 1) are one class of expanded porphyrins with five pyrrole rings joined with four *meso*-carbon bridges and one direct pyrrole bond and these macrocycles are oldest and simplest member of the expanded porphyrin family.[1–3] Sapphyrins are 22π electron aromatic macrocycles and were discovered serendipitously by Woodward and co-workers[3] during their pioneering work on synthesis of Vitamin B_{12}. The pentapyrrolic macrocycles were called sapphyrins because of their intense blue-colored crystals.[3] Although some work on sapphyrins have been reported in 1970's and 1980's, an intensification of interest in these macrocycles was generated when Sessler and co-workers[4] accidentally discovered in 1990's that these macrocycles can bind/sense anions, a feature that had not previously been recognized for porphyrinoid macrocycles. Sessler and co-workers[5] extensively investigated sapphyrin chemistry and developed facile methods for their synthesis, studied their aromatic character and their ability to bind metals and their specific versatile sensing ability of anions. Sapphyrins are also singlet-oxygen-producing photosensitizers and have been explored for potential applications in photodynamic therapy and viral photoeradication.[6] In addition, sapphyrins were also found to be potential compounds for treating leishmaniasis disease.[7] Because of their widespread applications, many structural variants of sapphyrins have been reported including *meso*-substituted sapphyrins,[8–11] carbasapphyrins,[6,12–16] heterosapphyrins, N- or heteroatom confused sapphyrins,[17] doubly N-confused sapphyrin derivatives,[13] sapphyrins incorporated with polycyclic aromatic hydrocarbons and so on.[13] Among many structural variants of sapphyrins, benzisapphyrins containing benzene and four pyrrole/heterocycle rings within a conjugated pathway is scarcely explored.[18] On the other hand, benzene-containing porphyrins have been extensively investigated by Lash et. al.[19,20] and other researchers and have shown that the benziporphyrins readily forms organometallic derivatives and have

potential applications in the development of chemical sensors and in molecular recognition studies.[8,21] Benziporphyrinoid macrocycles have been used to understand aromaticity and conjugation since the characteristics of benziporphyrinoids vary from nonaromatic to highly aromatic and in few cases antiaromatic structures are formed.[22–26] Thus, benzisapphyrins are highly desirable macrocycles to understand their diverse properties and applications. A perusal of literature revealed that there is only one report available on benzisapphyrins.[27] Sessler, Lee and co-workers[27] reported one example of dithia benzisapphyrin **2** (Chart 1) bearing exocyclic double bonds at the *meso*-positions which was obtained in 6% yield. The dithia analogue of *meso*-alkylidenyl sapphyrin **2** was nonaromatic since the conjugation pathway was interrupted by the *m*-phenylene unit.[27] Interestingly, this is the only report available on benzene-containing sapphyrin systems so far. However, the other reported dithia analogues of sapphyrins such as heterosapphyrins **3**-**5** (Chart 1) were found to be aromatic and showed interesting physico-chemical and anion sensing properties.[28] Therefore, it is interesting to design and synthesize benzene-containing sapphyrins so that they can be compared to previously reported aromatic heterosapphyrins **3**-**5**.[28] Furthermore, to the best of our knowledge, there is no report on benzene containing sapphyrins that are aromatic in nature. Thus, we made an attempt to design and synthesize aromatic dithia benzisapphyrins using readily available precursors. During our synthetic attempts, we realized that it is possible to synthesize aromatic dithia benzisapphyrins by changing the *m*-phenylene moiety to a *p*-phenylene unit. Herein, we report synthesis and properties of series of nonaromatic [24π] dithia *m*-benzisapphyrins **6**-**7** and aromatic [22π] dithia *p*-benzisapphyrins **8**-**10** which were prepared under simple acid catalyzed reaction conditions (Chart 2). The dithia *m*-benzisapphyrins and dithia *p*-benzisapphyrins exhibit quite different spectral and electrochemical properties from each other because of their differences in conjugation and aromaticity.

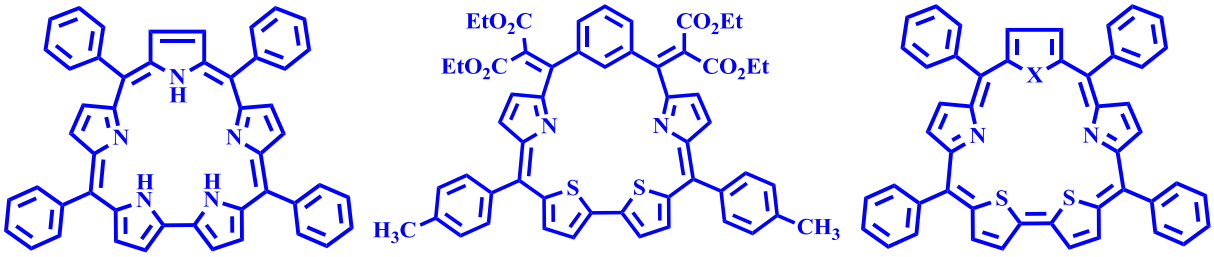

1 **2** **3; X=NH, 4; X=O, 5; X=S**

Chart 1: Structures of the sapphyrins and ditha *meta*-benzisapphyrin reported in the literature

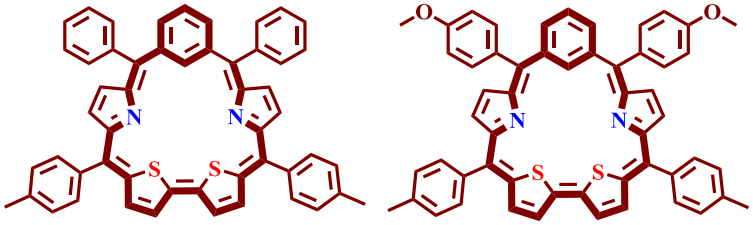

6 **7**

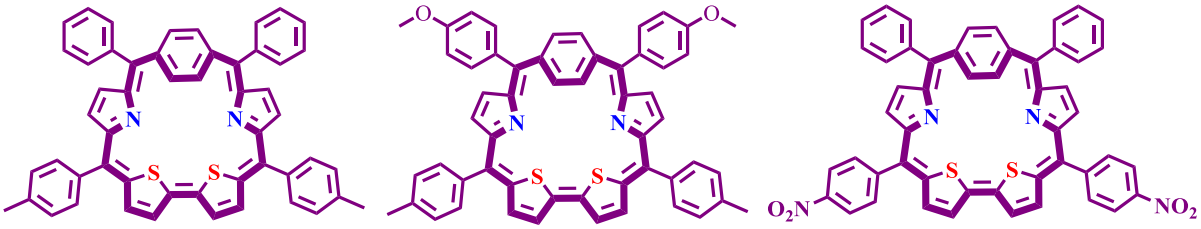

8 **9** **10**

Chart 2. Structures of the dithia *meta*-benzisapphyrins (**6** and **7**) and dithia *para*-benzisapphyrins (**8-10**).

Results and Discussion

Synthesis and characterization of dithia *m*-benzisapphyrins 6-7

Initially, we made an attempt to synthesize dithia *m*-benzisapphyrins by adopting 3+2 condensation approach. The desired diols **11a** and **11b** were prepared by treating isophthaldehyde with freshly prepared ArMgBr in THF followed by standard work up and

column chromatographic purification and afforded diols **11a** and **11b** as white solids in 65-70% yields.

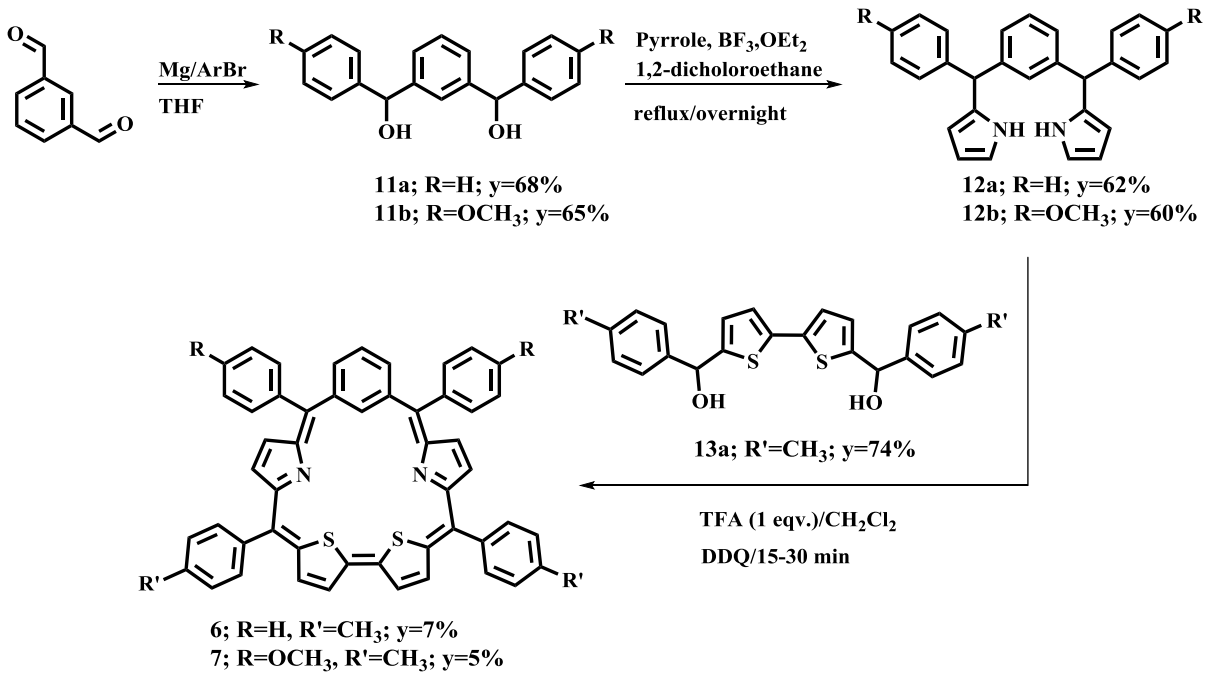

Scheme 1: Synthesis of ditha *m*-benzisapphyrins **6** and **7**.

The appropriate diols **11a/11b** were treated with pyrrole in 1,2-dichloroethane at reflux in the presence of catalytic amount of $BF_3.(OEt)_2$ followed by column chromatographic purification to afford the corresponding benzitripyrranes **12a/12b** in 60-65% yields. The other desired bithiophene diol **13a** was prepared by following the literature procedure.[29,30] All precursors were characterized by HR-MS, ^1H & ^{13}C NMR techniques. The dithia *m*-benzisapphyrins **6** and **7** were synthesized by condensing one equivalent of the appropriate benzitripyrrane **12a/12b** with one equivalent of bithiophene diol **13a** in CH_2Cl_2 at room temperature in the presence of one equivalent of TFA under inert atmosphere for about 30-45 min, followed by oxidation with DDQ in open air at room temperature for 30 min (Scheme 1). TLC analysis showed one major dark red spot corresponding to the desired

dithia *m*-benzisapphyrin macrocycle **6-7**. The crude compounds were subjected to basic alumina column chromatography and collected the dithia *m*-benzisapphyrin macrocycle **6-7** in 5-7% yields. The dithia *m*-benzisapphyrins **6-7** were freely soluble in common organic solvents and their identities were confirmed by molecular ion peak in HRMS and detailed 1D and 2D NMR spectroscopy.

The ^{1}H, ^{1}H-^{1}H COSY and NOESY NMR spectra of dithia *m*-benzisapphyrin **6** is presented in Figure 1. The proton assignments were made on the basis of their location, integration, coupling constants and cross-peak correlations observed in COSY and NOESY spectra. The macrocycle **6** is symmetrical and showed resonances for half of the macrocycle which were easily identified using 1D and 2D NMR spectroscopy. The selected chemical shifts (^{1}H) were tabulated in supporting Information (Table S1). The inner type *g* proton of *m*-phenylene unit appeared as broad singlet at 8.03 ppm, whereas type *e* and type *f* protons of *m*-phenylene unit appeared as multiplet in the region of 7.38-7.44 ppm and a triplet at 6.19 ppm, respectively. The *meso*-phenyl protons (type *j*, *k* and *l*) also appeared in the region of 7.38-7.62 ppm and merged with other proton resonances. The NMR spectrum of macrocycle **6** showed that the inner *meta*-phenylene –CH proton (type *g*) appeared at downfield region, whereas the outer *meta*-phenylene protons (type *e* and type *f*) appeared at upfield region supporting that the macrocycle **6** is nonaromatic in nature. The other dithia *meta*-benzisapphyrin **7** also showed similar nonaromatic NMR features (Figure S14).

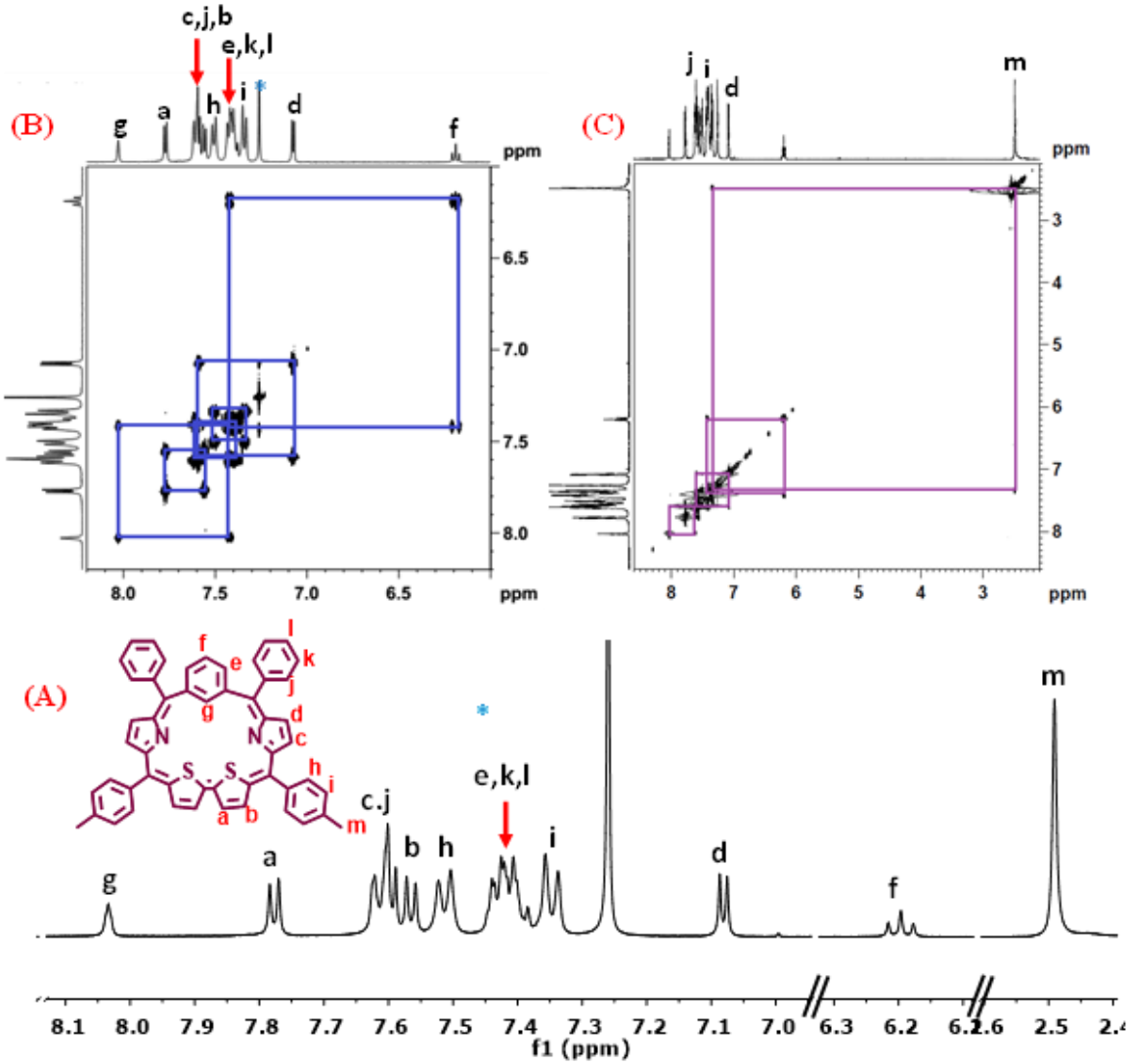

Figure 1: (A) Partial ^{1}H NMR spectra of compound **6**; Resonances were assigined on the basis of correlations observed in ^{1}H-^{1}H COSY (B) and ^{1}H-^{1}H NOESY (C) spectrum as shown in this figure.

Synthesis and characterization of dithia *p*-benzisapphyrins 8-10:

Since dithia *m*-benzisapphyrins **6-7** were found to be nonaromatic 24π electron systems, we thought that if we replace *m*-phenylene moiety of the macrocycle with *p*-phenylene moiety, the resulting *p*-benzisapphyrin macrocycle would be a 22π aromatic system like **1** and core-modified sapphyrins **3-5**.[28] With this idea in mind, we attempted the

synthesis of dithia *p*-benzisapphyrins **8-10** as shown in Scheme 2. The desired *p*-phenylene based diols **14a-14b** were synthesized by treating terephthaldehyde with freshly prepared ArMgBr in THF followed by work-up and column chromatographic purification yielded diols **14a-14b** in 65-70% yields. The corresponding *p*-benzitripyrranes **15a-15b** were prepared by treating appropriate diol **14a**/**14b** with excess pyrrole in 1,2-dichloroethane at reflux for overnight followed by column chromatographic purification to afford *p*-benzitripyrranes **15a-15b** in 60-65% yields.

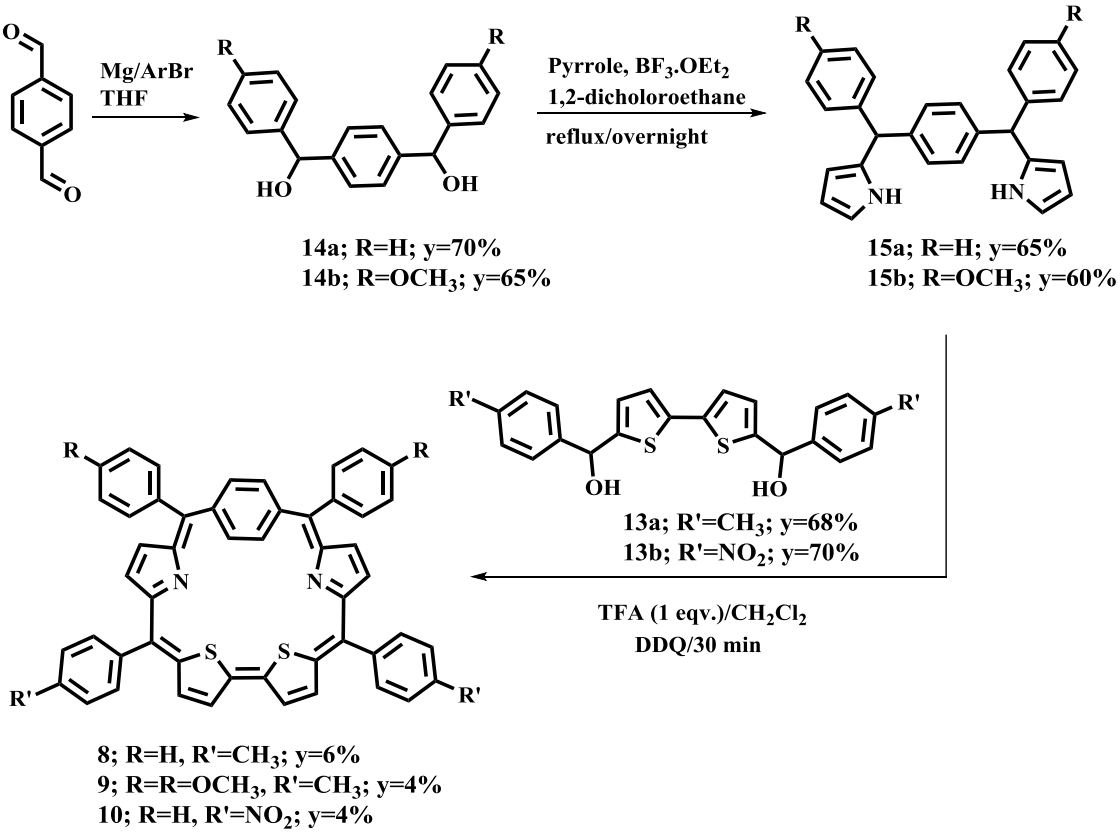

Scheme 2: Synthesis of ditha *p*-benzisapphyrins **8-10**.

The dithia *p*-benzisapphyrins **8-10** were synthesized by condensing one equivalent of *p*-benzitripyrrane **15a**/**15b** with one equivalent of bithiophene diol **13a**/**13b** in CH_2Cl_2 in the presence of one equivalent of TFA at room temperature for 1 h followed by oxidation with DDQ in open air for additional 30 min. TLC analysis showed one major spot corresponding to the required macrocycle along with trace amounts of one or two additional spots

corresponding to the unidentified products. The crude compound was subjected to basic alumina column chromatographic purification and afforded the pure dithia *p*-benzisapphyrins **8**-**10** in 4-6% yields.

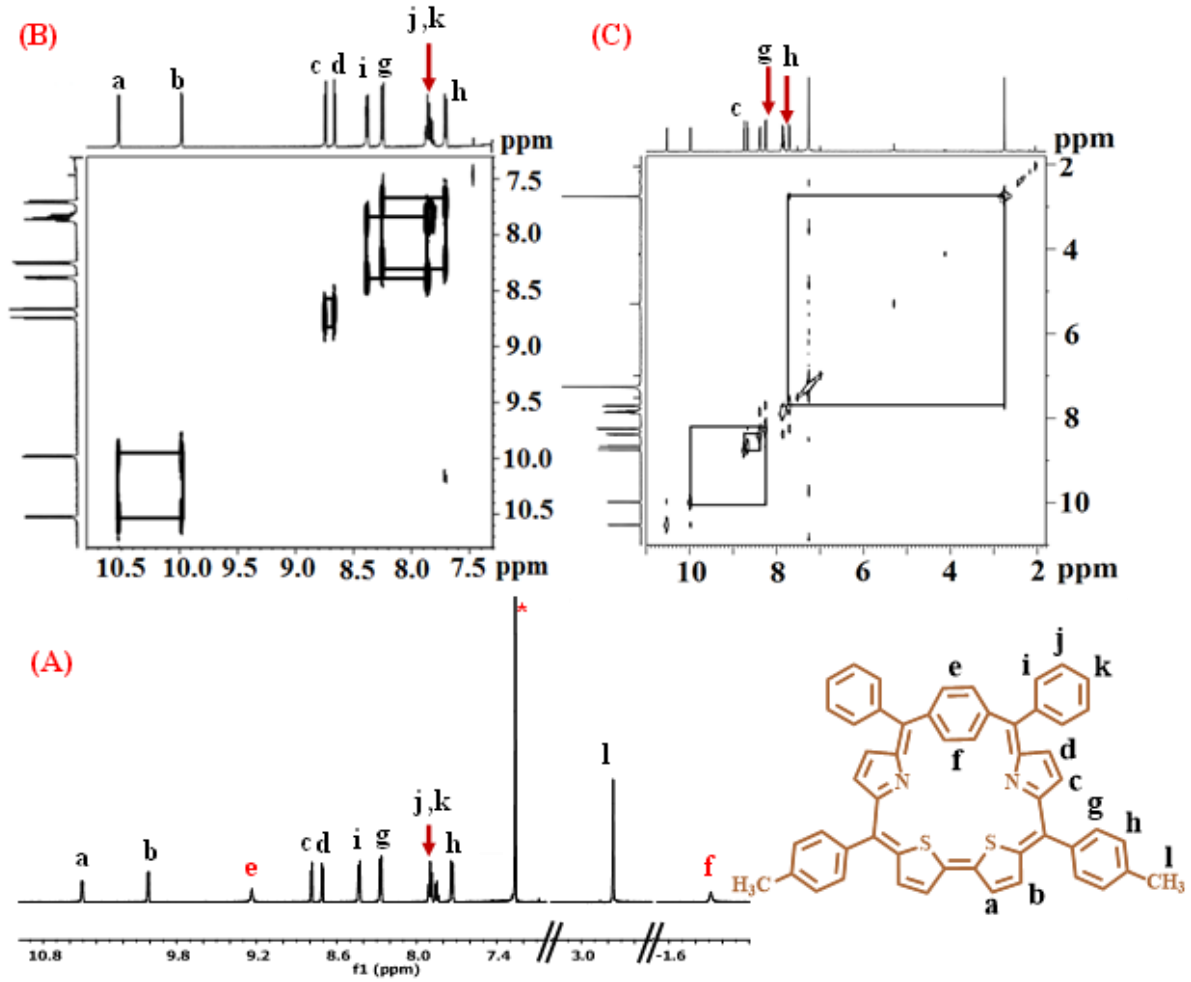

Figure 2: (A) Partial ^{1}H NMR spectra of the compound **8**; Resonances were assigined on the basis of correlations observed in ^{1}H-^{1}H COSY (B) and ^{1}H-^{1}H NOESY (C) spectrum as shown in this figure.

The molecular ion peak in HR-MS confirmed the identities of dithia *p*-benzisapphyrins **8**-**10**. Macrocycles **8**-**10** were thoroughly characterized by 1D and 2D NMR spectroscopy and ^{1}H, ^{1}H-1H COSY and NOESY NMR spectra of macrocycle **8** are presented in Figure 2. The ^{1}H NMR spectra of macrocycle **8** was very well resolved and all resonances were identified easily using cross peak correlations observed in 2D NMR. The selected peak

resonances for the compound **8** for comparion with compounds **6** and **4** were included in supporting information (Table S1). Interestingly, the four *p*-phenylene protons in macrocycle **8** were completely absent in the NMR spectrum recorded at room temperature due to its rapid rotation in NMR time scale. Hence, we recorded ^{1}H NMR and ^{1}H-^{1}H COSY spectra at -40 ºC to slow down the rotation of the *p*-phenylene ring in macrocycle **8**. In macrocycle **8**, the four protons of *p*-phenylene ring appeared as two sets of slightly broad singlets at -1.91 ppm (type *f*) and 9.24 ppm (type *e*). The other protons of macrocyclic ring showed almost negligible shifts at low temperature NMR compared to the room temperature NMR. Inspection of the dithia *p*-benzisapphyrin NMR clearly showed that the downfield shifts of outer ring protons and upfield shift of inner ring protons (Figure 2 and Table S1) supporting the operation of diatropic ring current effect and the aromatic nature of *p*-benziporphyrin macrocycle **8**. Furthermore, we compared the NMR features of *p*-benzisapphyrin macrocycle **8** with structurally analogous aromatic heterosapphyrin **4**. For example, in compound **4**, the type *a* and type *b* protons of bithiophene unit appeared as doublets at 9.40 and 9.75 ppm, respectively were downfield shifted in *p*-benzisapphyrin macrocycle **8** and appeared at 10.51 and 10.01 ppm, respectively. Similarly, the *β*-pyrrole protons (type *c* and type *d*) were more downfield shifted in macrocycle **8** compared to macrocycle **4**. In macrocycle **4**, the furan ring which was opposite to bithiophene unit was inverted and the *β*-protons of inverted furan ring which was under diatropic ring current effect appeared at 0.61 ppm whereas in *p*-benzisapphyrin macrocycle, the inner *p*-phenylene-protons appeared at -1.91 ppm. All these upfield and downfield shifts of various protons clearly indicated that the macrocycle **8** possesses more diatropic ring current than the structurally analogous heteroatom substituted sapphyrin **4**. The other two aromatic *p*-benzisapphyrin macrocycles **9** and **10** also showed similar NMR features like that of macrocycle **8** (Figures S21 and S24).

Absorption and electrochemical properties of *m*-benzisapphyrins and *p*-benzisapphyrins:

The absorption and electrochemical properties of dithia *m*-benzisapphyrins **6-7** and dithia *p*-benzisapphyrins **8-10** were investigated and the data are presented in Table 1. The comparison of absorption spectra of dithia *m*-benzisapphyrin **6** and dithia *p*-benzisapphyrin **8** recorded in toluene are shown in Figure 3A. The *m*-benzisapphyrin **6** showed an intense broad band at 397 nm along with a shoulder band at 493 nm and a broad less intense band at 823 nm supporting the nonaromatic nature of the macrocycle. Whereas, the *p*-benzisapphyrin **8** showed one intense sharp Soret like band at 484 nm along with three Q-type bands at 668, 762 and 854 nm which are in agreement with the aromatic nature of the macrocycle. We also carried out protonation titration of *m*-benzisapphyrin **6** and *p*-benzisapphyrin **8** by systematic addition of increasing amounts of TFA to the macrocycles **6** and **8** in toluene as shown in Figures 3B and 3C, respectively. Addition of increasing amounts of TFA to the solution of **6**, the colour of the solution was changed from yellow to dark brown due to formation of diprotonated species **6.2H**$^{2+}$ and the broad band at 397 nm was shifted bathochromically to relatively sharp intense band at 431 nm and the band at 823 nm was shifted to 1071 nm with two clear isosbestic points at 444 and 895 nm (Figure 3B). The compound **8** upon sequential addition of increasing amounts of TFA showed distinct colour change from red to pink and the resulting **8.2H**$^{2+}$ showed two bands at 507 and 806 nm and two clear isosbestic points at 493 and 703 nm were noted.

The redox properties of dithia *m*-benzisapphyrins **6-7** and dithia *p*-benzisapphyrins **8-10** were studied by cyclic voltammetry (CV) and differential pulse voltammetry (DPV) using 0.1 M tetrabutyl ammonium perchlorate (TBAP) as the supporting electrolyte in CH_2Cl_2. The comparison of reduction waves of compounds **6** and **8** are presented in Figure 3D and the relevant data for all compounds were included in Table 1.

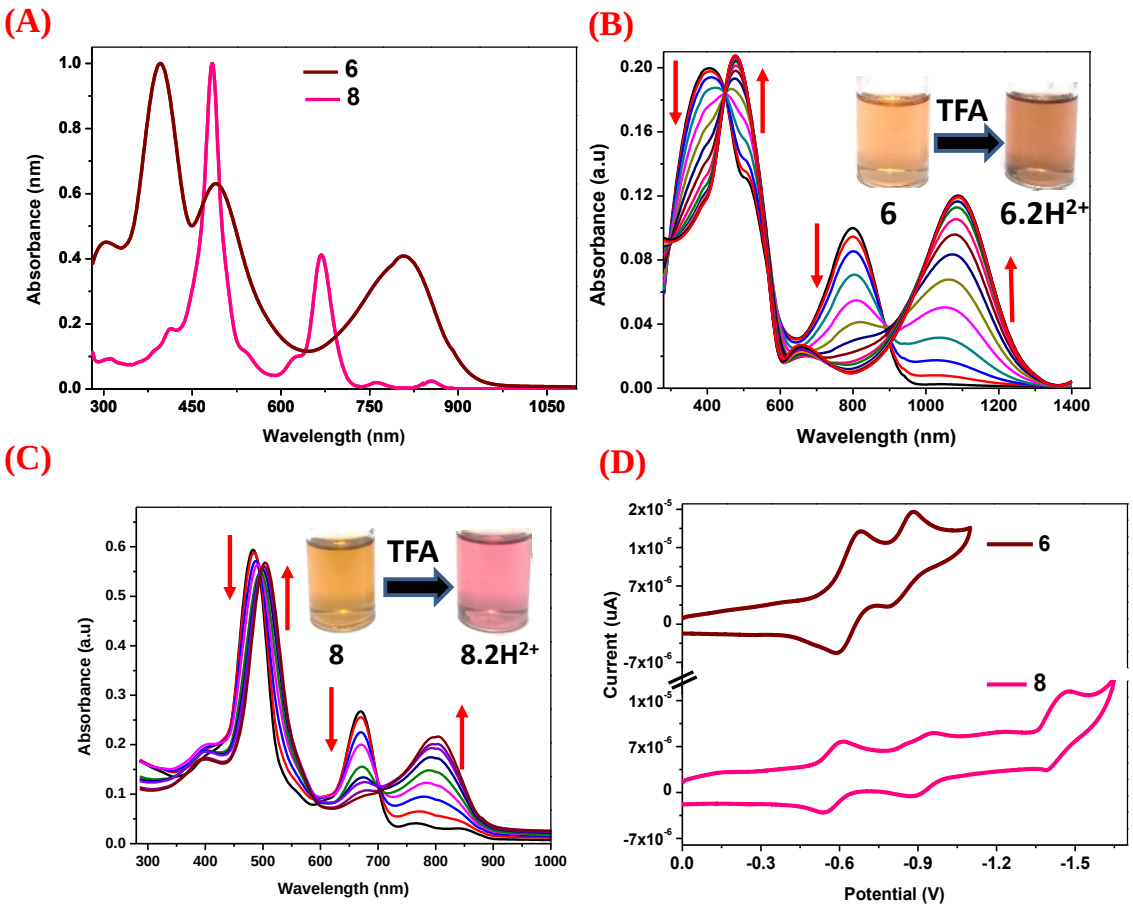

Figure 3: (A) Comparison of absorption spectra of the compounds **6** (brown line) and **8** (pink line) (5 µM) recorded in toluene, (B) Change in the absorption spectra of **6** upon the systematic addition of trifluoroacetic acid (0-150 eq.) in toluene, (C) Change in the absorption spectra of **8** upon the systematic addition of trifluoroacetic acid (0-90 eq.) in toluene, and (D) Comparison of cyclic voltamograms of compounds **6** (brown line) and **8** (pink line), recorded in CH_2Cl_2 containing 0.1 M TBAP as the supporting electrolyte and a saturated calomel electrode (SCE) as the reference electrode at scan rates of 50 mV s^{-1}.

Comparison of redox waves of all the compounds is included in supporting information (Figure S27). In general dithia *m*-benzisapphyrins **6-7** and dithia *p*-benzisapphyrins **8-10** showed two irreversible oxidations and two to three quasi-reversible/reversible reductions. For example, compound **6** showed two oxidations at 0.68 V, 1.14 V and two reductions at -

0.66 V and -0.88 V, whereas compound **8** showed two oxidations at 0.89 V, 1.35 V and three reductions at -0.60 V, -0.95 V and -1.46 V. A close inspection of redox data indicates that dithia *p*-benzisapphyrins **8-10** were difficult to oxidize but relatively easier to reduce compared to dithia *m*-benzisapphyrins **6-7**. The reversible nature of reduction waves noted for dithia *m*-benzisapphyrins **6-7** and dithia *p*-benzisapphyrins **8-10** indicates that these macrocycles are stable under reduction conditions.

Table 1: Absorption and electrochemical data of the compounds **6-10.**

Compound	Absorption data				Redox data				
	λ_1 nm (log ε)	λ_2 nm (log ε)	λ_3 nm (log ε)	λ_4 nm (log ε)	Oxidation (V)		Reduction (V)		
6	397 (4.77)	493 (sh)	823 (4.29)	-	1.14	0.68	-0.66	-0.88	-
6.2H^{2+}	431 (4.55)	503 (4.69)	1071 (4.26)	-	-	-	-	-	-
7	406 (4.58)	500 (sh)	837 (4.04)	-	1.00	0.62	-0.70	-0.92	-
7.2H^{2+}	451 (4.41)	567 (4.85)	1113 (3.98)	-	-	-	-	-	-
8	484 (5.14)	668 (4.75)	762 (3.37)	854 (3.47)	1.35	0.89	-0.60	-0.95	-1.46
8.2H^{2+}	507 (5.19)	806 (4.76)	-	-	-	-	-	-	-
9	487 (4.61)	676 (4.16)	767 (2.75)	858 (2.86)	1.31	0.82	-0.63	-0.95	-1.46
9.2H^{2+}	519 (4.59)	840 (4.23)	-	-	-	-	-	-	-
10	484 (4.71)	671 (4.32)	757 (2.95)	849 (2.49)	1.60	0.99	-0.50	-0.69	-0.97
10.2H^{2+}	504 (4.79)	803 (4.34)	-	-	-	-	-	-	-

DFT and TD-DFT studies:

DFT and TD-DFT studies were used to understand the structural and spectral characteristics of dithia *m*-benzisapphyrins **6-7** and dithia *p*-benzisapphyrins **8-10**. The geometry in S_0 state optimization, NICS (Nucleus-Independent Chemical Shifts)[31,32] and AICD (Anisotropy Induced Current Density)[33] calculations for the representative compounds **6** and **8** were performed using with B3LYP/6-31g(d,p) level of theory. The optimized structures of the compounds **6** and **8** are presented in Figure 4. The DFT studies revealed distorted structure for the dithia *m*-benzisapphyrin **6** with *m*-phenylene moiety deviated from the mean plane (defined by four *meso* carbon atoms) to great extent as shown in Figure 4 (a, b). Whereas, the macrocyclic core of the dithia *p*-benzisapphyrin **8** showed an almost planar arrangement, except the *p*-phenylene ring which deviated from the mean plane (defined by four *meso* carbons) by 21.9 ° (Figures 4c and 4d).

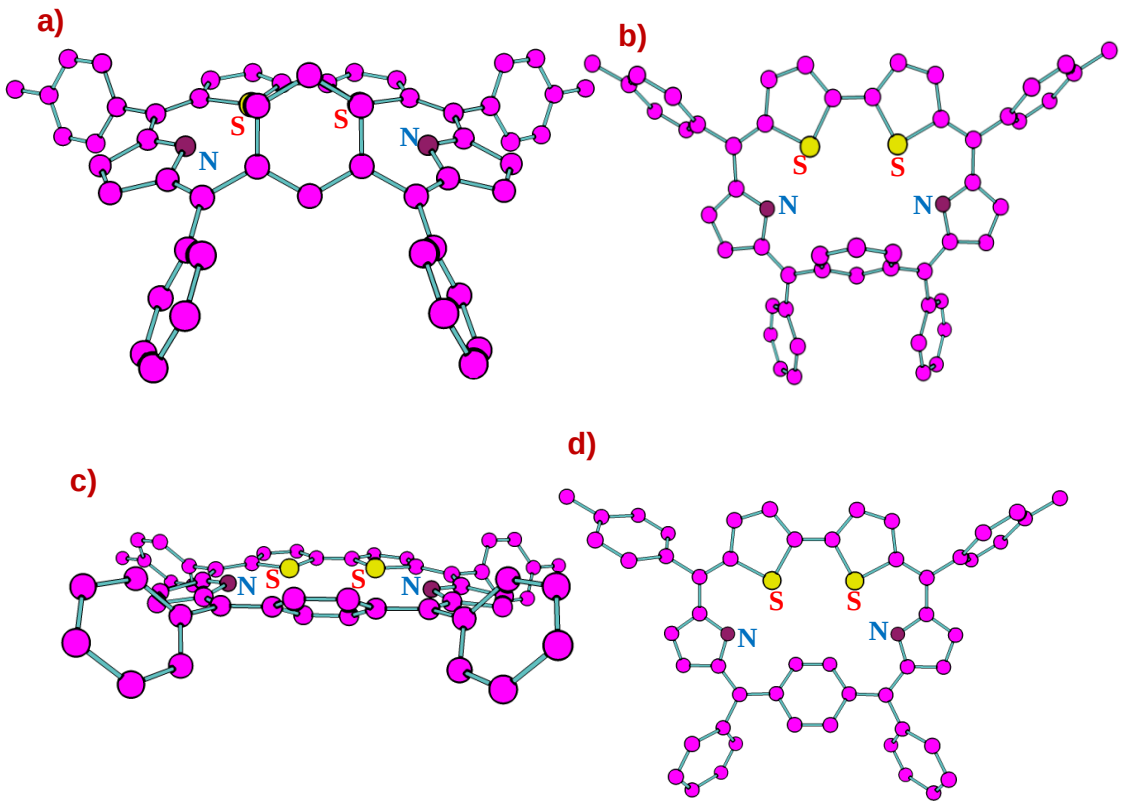

Figure 4. DFT (B3LYP/6-31g(d,p)) optimized structures of the compound **6** ((a)-side view and (b) top view) and compound **8** ((c)-side view and (d) top view).

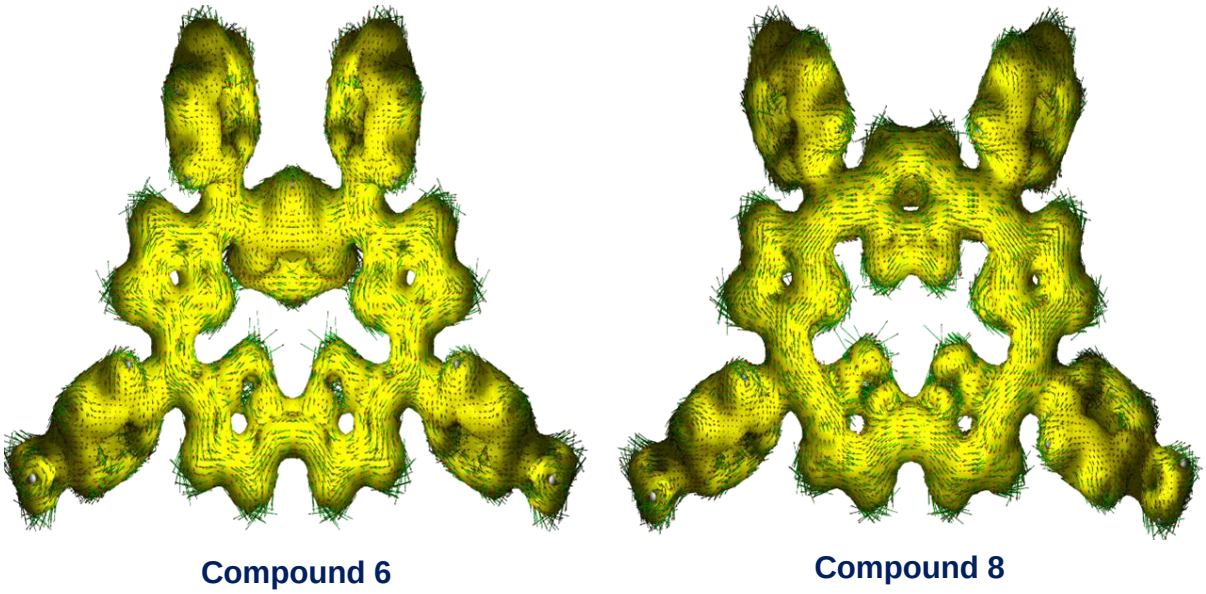

Figure 5. AICD plots of the compounds **6** and **8**.

The AICD plot (Figure 5) of the compound **6** displayed the clockwise ring current which was interrupted at *m*-phenylene moiety of the macrocyclic core favoring nonaromatic character of the compound **6**. Whereas the AICD plot of the compound **8** displayed continuous clockwise ring current favouring aromatic character of the macrocycle **8** which was also supported by the NICS(0) value of -13.48 ppm.

The analysis of frontier molecular orbitals revealed that the HOMO of the compound **6** was much more destabilized compared to that of the compound **8**, whereas the LUMO of the compound **6** was stabilized to some extent compared to that of compound **8** (Figure 6). This leads to the decrease in the band gap (ΔE = E_{LUMO}-E_{HOMO}) for the compound **6** (ΔE = 0.587 eV) compared to that of compound **8** (ΔE = 0.948 eV), supporting the observed red shift in

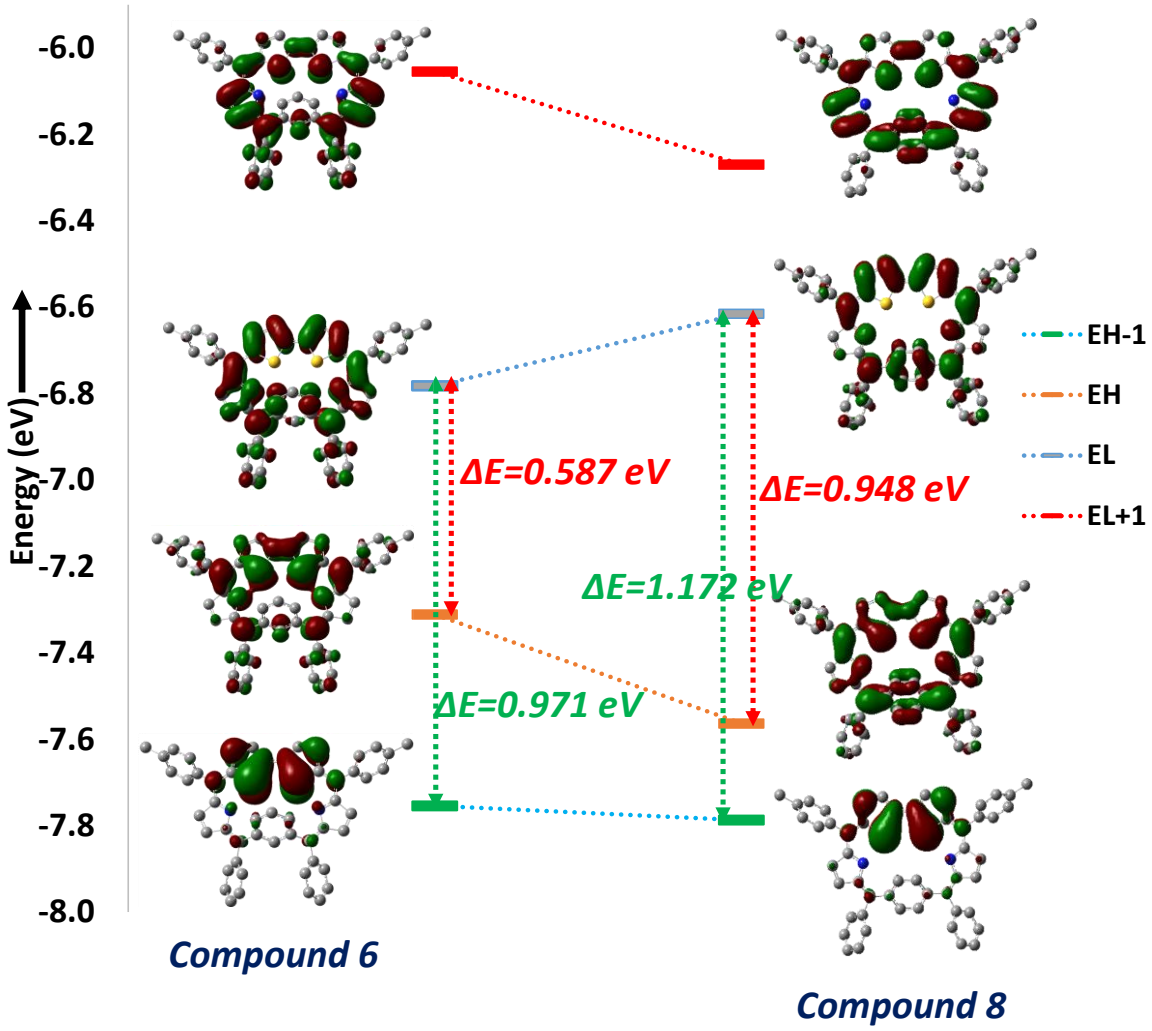

Figure 6. Energy level diagram (selected frontier molecular orbitals) of the compounds **6** and **8** calculated by DFT (B3LYP/6-31g(d,p)) method; (E_{H-1}= Energy of HOMO-1; E_H= Energy of HOMO; E_L= Energy of LUMO; and E_{L+1}= Energy of LUMO+1 orbitals).

the absorption of dithia *m*-benzisapphyrins **6-7** compared to that of dithia *p*-benzisapphyrins **8-10**. The analysis of the FMOs of the compound **6** suggest the transfer of charge from one part of the molecule to another.

Further, the TD-DFT studies were carried out to evaluate the excitation energies and oscillator strengths for first 50 S_0-S_n transitions and comparison of calculated excitation energies (black vertical lines) and experimental UV-Vis spectra (colored lines) is presented in

Figure S28. The oscillator strengths (right axes) for the compounds **6** and **8** represents the probability of the occurrence of corresponding transitions and are proportional to the molar extinction coefficients (left axes) found for the compounds **6** and **8**. From figure S28 it is seen that, the TD-DFT studies suggested very close match between the observed and calculated absorption spectra for the compounds **6** and **8**. The HOMO→LUMO transitions were responsible for the observed low energy charge transfer band and Q bands in compounds **6** and **8**, respectively. It is clear from the figure 6 that the HOMO-1 orbital of the compound **6** was destabilized compared to that of compound **8**. This resulted in the decrease of the E_L–E_{H-1} gap for compound **6** which reflected in its red shifted low energy absorption band compared to that of compound **8**.

Conclusions:

In conclusion, we prepared a series of benzisapphyrins by 3+2 condensation of appropriate benzitripyrrane with bithiophene diol under acid catalysed conditions. We showed that the dithia benzisapphyrins can be made aromatic by replacing *m*-phenylene moiety of the macrocycle with *p*-phenylene moiety using NMR, absorption, redox and DFT studies. The studies also indicated that the dithia *p*-benzisapphyrins are relatively more aromatic in nature compared to the reported hetero sapphyrins. Metalation and sensing studies of these new aromatic *meso*-aryl dithia *p*-benzisapphyrins are currently under investigation.

Experimental Section

General Experimental: The chemicals such as $BF_3{\cdot}OEt_2$, 2, 3-dichloro-5, 6-dicyano-1, 4-benzoquinone (DDQ) were used as obtained from Aldrich. All other chemicals used for the synthesis were reagent grade unless otherwise specified. Column chromatography was

performed on silica gel and basic alumina. Compounds **11a-11b**[34], **12a-12b**[35], **13a-13b**[29,30], **14a-14b**[23,36,37], **15a-15b**[23] were synthesized by the reported methods. The ^{1}H, and ^{13}C NMR spectra were recorded in $CDCl_3$ on Bruker 400 and 500 MHz instruments. The frequencies for ^{13}C nucleus are 100.06 and 125.77 MHz for 400 MHz and 500 MHz instruments respectively. Tetramethylsilane [Si $(CH_3)_4$] was used as an internal standard for ^{1}H and ^{13}C NMR. Absorption spectra were obtained with Shimadzu UV-Vis-NIR Spectrophotometer. Cyclic voltammetry (CV) studies were carried out with BAS electrochemical system utilizing the three electrode configuration consisting of a glassy carbon (working electrode), platinum wire (auxiliary electrode) and saturated calomel (reference electrode) electrodes. The experiments were done in dry dichloromethane using 0.1 M tetrabutylammonium perchlorate as supporting electrolyte. The HR mass spectra were recorded with a Q-Tof micro mass spectrometer.

Computational details: All the calculations were done using of the Gaussian 09 program package.[38] The density functional theory (DFT)[39] method; hybrid functional B3LYP in conjunction with basis set 6-31G(d,p),[40] was used to optimizes the structures of the compounds **6** and **8** in ground (S0) states. Using same hybrid functional and basis set the vertical excitation energies and oscillator strengths were obtained for the 50 lowest $S_0 \rightarrow S_n$ transitions at the optimized S_0 state equilibrium geometries using time dependant density functional theory (TD-DFT) method.[41–49] All the computations in the toluene media were carried out using the Self-Consistent Reaction Field (SCRF) under the Polarisable Continuum Model (PCM).[50,51] The electronic absorption spectra, including oscillator strengths were systematically investigated using TD-DFT with PCM model on the basis of the S_0 optimized structures.

Synthesis of 1,3-benzene-bis((4-methoxyphenyl)methanol (11b).

The solution of isophthalaldehyde (1.00 g, 7.46 mmol) in dry THF (100 mL) was cooled to 0 ° C and freshly prepared anisyl magnesium bromide (22 mL in THF, 44.74 mmol) was added to it by maintaining reaction temperature at 0 °C under N_2 atmosphere. The resulting mixture was stirred at room temperature for 2 h and the mixture was slowly poured on to the ice cold aqueous ammonium chloride solution. The resulting mixture was extracted with diethyl ether (70 mL x 3) and the combined organic layers were dried over anhydrous sodium sulphate. The crude compound obtained after removal of solvent under vacuum was subjected to silica gel (100-200) column chromatography using pet ether and ethyl acetate (40:60 v/v) and the desired product **11b** was obtained as white semi-solid in 65% yield (1.69 g). ^{1}H NMR (500 MHz, $CDCl_3$) δ 7.43-7.46 (m, *J* = 9.9 Hz, 1H), 7.23 – 7.31 (m, 7H), 6.84 (d, *J* = 8.6 Hz, 4H), 5.76 (s, 2H), 3.80 (s, 6H), 2.53 (s, 2H). ^{13}C NMR (126 MHz, $CDCl_3$) δ 159.1, 144.4, 144.3, 136.2, 129.3, 128.6, 128.1, 128.0, 125.7, 125.6, 124.5, 114.0, 113.3, 75.8, 55.4. HRMS (ESI): calcd. for $C_{22}H_{21}O_3$ $[M-OH]^+$ m/z 333.1485; found m/z 333.1494.

Synthesis of 1,3-bis((4-methoxyphenyl)(1H-pyrrol-2-yl)methyl)benzene (12b).

To the solution of **11b** (1.00 g, 2.86 mmol) and pyrrole (20 mL) in 1, 2-dichloroethane (40 mL), $BF_3{\cdot}Et_2O$ (1.5 mL) was added and the resulting mixture was stirred under N_2 atmosphere at reflux for 16 h. The reaction mixture was then cooled to room temperature and quenched by addition 2N sodium hydroxide solution (100 mL). The mixture was extracted using dichloromethane (50 mL x 3) and combined organic layers were dried on anhydrous sodium sulphate. The solvent and excess pyrrole were removed using high vacuum. The black semisolid obtained was purified by column chromatography on silica gel, eluting with pet ether and dichloromethane (60:40) mixture to afford pure compound **12b** as pale yellow semi-solid. The NMR data were consistent with the presence of two

diastereomers. Yield- 0.77 g, (60%); ^{1}H NMR (400 MHz, $CDCl_3$) δ 7.77 (s, 2H), 7.22 (t, *J* = 7.6 Hz, 1H), 7.07 – 6.96 (m, 7H), 6.82 (d, *J* = 8.6 Hz, 4H), 6.67 (s, 2H), 6.13 (dd, 2H), 5.75 (s, 2H), 5.34 (s, 2H), 3.79 (s, 6H). ^{13}C NMR (126 MHz, $CDCl_3$) δ 158.3, 143.7, 135.3, 134.1, 131.3, 129.9, 129.5, 128.7, 127.1, 127.0, 117.2, 113.9, 112.9, 108.2, 107.8, 55.3, 49.8, 49.7. HRMS (ESI): calcd. for $C_{30}H_{28}KN_2O_2$ $[M + K]^+$ m/z 487.1782; found m/z 487.1781.

Synthesis of [2,2'-bithiophene]-5,5'-diylbis((4-nitrophenyl)methanol (13b).

Dry and distilled *n*-hexane (30 mL) was added to a 250 mL three-necked round-bottom flask containing 2,2'-bithiophene (1.00 g, 6.02 mmol) which was equipped with a glass inlet tube, a reflux condenser and a rubber septum. N,N,N',N'-Tetramethyl ethylene diamine (2.25 mL, 15.06 mmol) and *n*-BuLi (9.00 mL of 1.6 M solution in *n*-hexane) were injected into the stirred solution and refluxed for 1h. The reaction mixture was then allowed to attain room temperature and cooled to 0 °C. The ice-cold solution of *p*-nitrobenzaldehyde (1.52 mL, 15.06 mmol) in dry THF (30 mL) was added drop wise to the reaction mixture. After the addition was complete, the reaction mixture was allowed to attain room temperature. After 15-20 min, saturated ammonium chloride solution was added and the resulting mixture was extracted with diethyl ether (50 mL x 3). The combined organic layers were washed with brine water and dried over anhydrous Na_2SO_4. The crude compound obtained after removal of solvent was subjected to silica gel column chromatography using petroleum ether/ethyl acetate (65:35) and the desired diol **13b** was collected as white solid. Yield- 70% (1.97 g); mp. 160-162° C; ^{1}H NMR (500 MHz, $CDCl_3$) δ 8.22 (d, *J* = 8.8 Hz, 4H), 7.63 (d, *J* = 8.4 Hz, 4H), 6.96 (d, 2H), 6.83 (d, *J* = 3.6 Hz, 2H), 6.11 (s, 2H), 2.70 (s, 2H). ^{13}C NMR (126 MHz, $CDCl_3$) δ 149.6, 147.7, 145.9, 138.0, 127.1, 126.4, 124.0, 123.6, 71.5. HRMS (ESI): calcd. for $C_{22}H_{16}NaN_2O_6S_2$ $[M + Na]^+$ m/z 491.0342; found m/z 491.0349.

General procedure for synthesis of dithia benzisapphyrins (6-10).

To the solution of appropriate tripyrrane (0.50 mmol) in dichloromethane under N_2 atmosphere, appropriate *bis*-thiophene dicarbinol **13a/13b** (0.50 mmol) was added and resulting mixture was stirred at room temperature until dicarbinol was completely dissolved. Trifluoroacetic acid (TFA) (0.50 mmol) was added to initiate the condensation and the reaction mixture was stirred at room temperature under inert atmosphere for 30-45 min. DDQ (1.25 mmol) was then added and the reaction mixture was stirred at room temperature in open air for additional 30 min. After completion of reaction as judged by TLC and UV-Vis spectroscopy, the solvent was removed on a rotary evaporator under vacuum. The resulting crude compounds were purified by basic alumina column chromatography using pet ether-dichloromethane (80:20) as eluent and the desired dithia *m*-benzisapphyrins (**6-7**) and dithia *p*-benzisapphyrins (**8-10**) were obtained as dark brown solids in 4-7% yields.

Synthesis of compound 6

The compound **6** was synthesized from **12a** (194 mg, 0.50 mmol) and **13a** (203 mg, 0.50 mmol) by following general procedure reported above for compounds **6-10;** Yield- 7% (26 mg); mp. >300° C; ^{1}H NMR (400 MHz, $CDCl_3$, in ppm) δ 8.03 (s, 1H), 7.78 (d, *J* = 5.5 Hz, 2H), 7.59-7.62 (m, 6H), 7.56 (d, *J* = 5.5 Hz, 2H), 7.51 (d, *J* = 7.5 Hz, 4H), 7.38-7.44 (m, 8H), 7.35 (d, *J* = 7.9 Hz, 4H), 7.08 (d, *J* = 4.6 Hz, 2H), 6.19 (t, *J* = 7.8 Hz, 1H), 2.49 (s, 6H). ^{13}C NMR (126 MHz, $CDCl_3$, in ppm)) δ 145.5, 139.6, 138.6, 137.4, 134.9, 133.3, 131.4, 129.9, 129.3, 129.1, 128.4, 125.6, 21.5. HRMS (ESI): calcd. for $C_{52}H_{37}N_2S_2$ $[M + H]^+$ m/z 753.2393; found m/z 753.2452.

Synthesis of compound 7

The compound **7** was synthesized from **12b** (224 mg, 0.50 mmol)) and **13a** (203 mg, 0.50 mmol) by following general procedure given above for compounds **6-10;** Yield- 5% (20 mg); mp. >300° C; ^{1}H NMR (400 MHz, $CDCl_3$) δ 8.12 (s, 1H), 7.74 (d, *J* = 5.5 Hz, 2H), 7.57 – 7.59 (m, 6H), 7.50-7.53 (m, *J* = 7.0 Hz, 6H), 7.42 (dd, *J* = 7.8, 1.7 Hz, 2H), 7.34 (d, *J* = 7.8 Hz, 4H), 7.07 (d, *J* = 4.9 Hz, 2H), 6.97 (d, *J* = 7.1 Hz, 4H), 6.21 (t, *J* = 7.8 Hz, 1H), 3.88 (s, 6H), 2.49 (s, 6H). ^{13}C NMR (101 MHz, $CDCl_3$) δ 161.0, 138.6, 137.3, 134.8, 134.6, 131.4, 129.3, 129.1, 125.6, 114.0, 55.6, 29.8. HRMS (ESI): calcd. for $C_{54}H_{41}N_2O_2S_2$ $[M + H]^+$ m/z 813.2604; found m/z 813.2603.

Synthesis of compound 8

The compound **8** was synthesized from **15a** (194 mg, 0.50 mmol) and **13a** (203 mg, 0.50 mmol) by following general procedure reported above for compounds **6-10;** Yield- 6% (22 mg); mp. >300° C; ^{1}H NMR (600 MHz, $CDCl_3$, -40° C) δ 10.51 (d, *J* = 4.8 Hz, 2H), 10.01 (d, *J* = 4.8 Hz, 2H), 9.24 (s, 2H), 8.79 (d, *J* = 4.3 Hz, 2H), 8.71 (d, *J* = 4.3 Hz, 2H), 8.43 (d, *J* = 6.8 Hz, 4H), 8.27 (d, *J* = 7.6 Hz, 4H), 7.84–7.91 (m, 6H), 7.74 (d, *J* = 7.5 Hz, 4H), 2.76 (s, 6H), -1.91 (s, 2H). ^{13}C NMR (101 MHz, $CDCl_3$) δ 159.4, 155.8, 144.0, 143.6, 141.1, 140.1, 138.2, 138.0, 137.7, 135.8, 134.5, 131.6, 130.1, 128.8, 128.2, 128.1, 127.4, 21.7. HRMS (ESI): calcd. for $C_{52}H_{37}N_2S_2$ $[M + H]^+$ m/z 753.2393; found m/z 753.2389.

Synthesis of compound 9

The compound **9** was synthesized from **15b** (224 mg, 0.50 mmol) and **13a** (203 mg, 0.50 mmol) by following general procedure reported above for compounds **6-10;** Yield- 4% (16

mg); mp. >300° C; ^{1}H NMR (600 MHz, $CDCl_3$, -40° C) δ 10.44 (d, *J* = 4.9 Hz, 2H), 9.94 (d, *J* = 4.8 Hz, 2H), 9.17 (s, 2H), 8.77 (d, *J* = 4.3 Hz, 2H), 8.66 (d, *J* = 4.3 Hz, 2H), 8.40 (d, *J* = 8.3 Hz, 4H), 8.26 (d, *J* = 7.6 Hz, 4H), 7.72 (d, *J* = 7.6 Hz, 4H), 7.45 (d, *J* = 8.4 Hz, 4H), 4.15 (s, 6H), 2.76 (s, 6H), -1.64 (s, 2H). ^{13}C NMR (126 MHz, $CDCl_3$) δ 160.1, 159.6, 156.0, 143.5, 141.4, 140.1, 139.1, 138.3, 137.9, 137.6, 137.1, 135.5, 134.4, 131.2, 129.7, 128.8, 128.0, 113.1, 55.8, 29.8. HRMS (ESI): calcd. for $C_{54}H_{41}N_2O_2S_2$ $[M + H]^+$ m/z 813.2604; found m/z 813.2596.

Synthesis of compound 10

The compound **10** was synthesized from **15a** (194 mg, 0.50 mmol) and **13b** (234 mg, 0.50 mmol) by following general procedure reported above for compounds **9-10;** Yield- 4% (17 mg); mp. >300° C; ^{1}H NMR (600 MHz, $CDCl_3$, -40° C) δ 10.43 (d, *J* = 4.4 Hz, 2H), 9.76 (d, *J* = 4.6 Hz, 2H), 9.10 (s, 2H), 8.77 (m, 6H), 8.47-8.49 (m, *J* = 6.7 Hz, 6H), 8.38 (d, *J* = 6.6 Hz, 4H), 7.95 – 7.86 (m, 6H), -1.32 (s, 2H). ^{13}C NMR (101 MHz, $CDCl_3$) δ 159.1, 155.7, 148.0, 147.6, 143.8, 143.5, 143.2, 140.3, 138.8, 138.6, 135.8, 134.9, 130.5, 129.2, 128.6, 127.6, 126.4, 123.2. HRMS (ESI): calcd. for $C_{50}H_{31}N_4O_4S_2$ $[M + H]^+$ m/z 815.1781; found m/z 815.1792.

Associated Content

Supporting Information

HRMS spectra, spectral, electrochemical and computational data is included in supporting information. This material is available free of charge via the Internet at http:// pubs.acs.org.

Author Information

Corresponding Author

*E-mail: ravikanth@chem.iitb.ac.in.

Author Contributions

† R.S. and K.G.T. contributed equally.

Acknowledgements

M.R thanks the Department of Science and Technology, Govt. of India (File No. EMR/2015/002196 to M.R.) R.S. thanks the CSIR India for research fellowship and K.G.T thanks to IIT Bombay for a post-doctoral fellowship.

References:

(1) Broadhurst, M. J.; Grigg, R.; Johnson, A. W. The Synthesis of 22 π-Electron Macrocycles. Sapphyrins and Related Compounds. *J. Chem. Soc. Perkin Trans. 1* **1972**, *0*, 2111–2116.

(2) Sessler, J. L.; Cyr, M. J.; Lynch, V.; McGhee, E.; Ibers, J. A. Synthetic and Structural Studies of Sapphyrin, a 22-;π-Electron Pentapyrrolic "Expanded Porphyrin." *J. Am. Chem. Soc.* **1990**, *112* (7), 2810–2813.

(3) Bauer, V. J.; Clive, D. L. J.; King, M. M.; Dolphin, D.; Harris, F. L.; Loder, J.; Wang, S. W. C.; Paine, J. B.; Woodward, R. B. Sapphyrins: Novel Aromatic Pentapyrrolic Macrocycles. *J. Am. Chem. Soc.* **1983**, *105* (21), 6429–6436.

(4) Sessler, J. L.; Davis, J. M. Sapphyrins: Versatile Anion Binding Agents. *Acc. Chem. Res.* **2001**, *34* (12), 989–997.

(5) Burrell, A. K.; Sessler, J. L.; Cyr, M. J.; McGhee, E.; Ibers, J. A. Metal Carbonyl Complexes of Sapphyrins. *Angew. Chem. Int. Ed. Engl.* **1991**, *30* (1), 91–93.

(6) Král, V.; Davis, J.; Andrievsky, A.; Kralová, J.; Synytsya, A.; Poucková, P.; Sessler, J. L. Synthesis and Biolocalization of Water-Soluble Sapphyrins. *J. Med. Chem.* **2002**, *45* (5), 1073–1078.

(7) Hooker, J. D.; Nguyen, V. H.; Taylor, V. M.; Cedeño, D. L.; Lash, T. D.; Jones, M. A.; Robledo, S. M.; Vélez, I. D. New Application for Expanded Porphyrins: Sapphyrin and Heterosapphyrins as Inhibitors of Leishmania Parasites. *Photochem. Photobiol.* **2012**, *88* (1), 194–200.

(8) Srinivasan, A.; Anand, V. G.; Jeyaprakash Narayanan, S.; Pushpan, S. K.; Ravi Kumar, M.; Chandrashekar, T. K.; Sugiura, K. I.; Sakata, Y. Structural Characterization of Meso Aryl Sapphyrins. *J. Org. Chem.* **1999**, *64* (23), 8693–8697.

(9) Bruckner, C.; D. Sternberg, E.; W. Boyle, R.; Dolphin, D. 5,10-Diphenyltripyrrane, a Useful Building Block for the Synthesis of Meso-Phenyl Substituted Expanded Macrocycles. *Chem. Commun.* **1997**, No. 17, 1689–1890.

(10) Chandrashekar, T. K.; Venkatraman, S. Core-Modified Expanded Porphyrins: New Generation Organic Materials. *Acc. Chem. Res.* **2003**, *36* (9), 676–691.

(11) Sessler, J. L.; Lisowski, J.; Boudreaux, K. A.; Lynch, V.; Barxy, J.; Kodadek, T. J. Synthesis and Characterization of Diaryl Sapphyrins Prepared under Lindsey-Type Conditions. *J. Org. Chem.* **1995**, *60* (18), 5975–5978.

(12) Richter, D. T.; Lash, T. D. Synthesis of Sapphyrins, Heterosapphyrins, and Carbasapphyrins by a "4 + 1" Approach. *J. Org. Chem.* **2004**, *69* (25), 8842–8850.

(13) Sessler, J. L.; Cho, D. G.; Stępień, M.; Lynch, V.; Waluk, J.; Yoon, Z. S.; Kim, D. Inverted Sapphyrin: A New Family of Doubly N-Confused Expanded Porphyrins. *J. Am. Chem. Soc.* **2006**, *128* (39), 12640–12641.

(14) Lash, T. D. Modification of the Porphyrin Chromophore by Ring Fusion: Identifying Trends Due to Annelation of the Porphyrin Nucleus. *J. Porphyr. Phthalocyanines* **2001**, *5* (3), 267–288.

(15) Paolesse, R.; Licoccia, S.; Spagnoli, M.; Boschi, T.; Khoury, R. G.; Smith, K. M. A Novel Synthetic Route to Sapphyrins. *J. Org. Chem.* **1997**, *62* (15), 5133–5137.

(16) Panda, P. K.; Kang, Y. J.; Lee, C. H. A Benzodipyrrole-Derived Sapphyrin. *Angew. Chem. Int. Ed.* **2005**, *44* (26), 4053–4055.

(17) Gupta, I.; Srinivasan, A.; Morimoto, T.; Toganoh, M.; Furuta, H. N-Confused and N-Fused Meso-Aryl Sapphyrins. *Angew. Chem. Int. Ed.* **2008**, *47* (24), 4563–4567.

(18) Jeong, S. D.; Hong, S. J.; Kee, J. P.; Ham, S.; Sessler, J. L.; Lynch, V.; Lee, C. H. Core-Modified, Meso-Alkylidenyl Porphyrins and Their Expanded Analogues: A New Family of Nonplanar Porphyrinoids. *J. Org. Chem.* **2007**, *72* (16), 6232–6240.

(19) Muckey, M. A.; Szczepura, L. F.; Ferrence, G. M.; Lash, T. D. Silver(III) Carbaporphyrins: The First Organometallic Complexes of True Carbaporphyrins. *Inorg. Chem.* **2002**, *41* (19), 4840–4842.

(20) Liu, D.; Ferrence, G. M.; Lash, T. D. Oxybenziporphyrins, Oxypyriporphyrins, Benzocarbaporphyrins, and Their 23-Oxa and 23-Thia Analogues: Synthesis, Spectroscopic Characterization, Metalation, and Structural Characterization of a Palladium(II) Organometallic Derivative. *J. Org. Chem.* **2004**, *69* (18), 6079–6093.

(21) Stępień, M.; Latos-Grazyński, L.; Szterenberg, L.; Panek, J.; Latajka, Z. Cadmium(II) and Nickel(II) Complexes of Benziporphyrins. A Study of Weak Intramolecular Metal-Arene Interactions. *J. Am. Chem. Soc.* **2004**, *126* (14), 4566–4580.

(22) Lash, T. D. Benziporphyrins, a Unique Platform for Exploring the Aromatic Characteristics of Porphyrinoid Systems. *Org. Biomol. Chem.* **2015**, *13* (29), 7846–7878.

(23) Stępień, M.; Szyszko, B.; Latos-Grazyński, L. Steric Control in the Synthesis of P-Benziporphyrins. Formation of a Doubly n-Confused Benzihexaphyrin Macrocycle. *Org. Lett.* **2009**, *11* (17), 3930–3933.

(24) Stępień, M.; Latos-Grazyński, L.; Sprutta, N.; Chwalisz, P.; Szterenberg, L. Expanded Porphyrin with a Split Personality: A Hückel-Möbius Aromaticity Switch. *Angew. Chem. Int. Ed.* **2007**, *46* (41), 7869–7873.

(25) Szyszko, B.; Sprutta, N.; Chwalisz, P.; Stępień, M.; Latos-Grazyński, L. Hückel and Möbius Expanded Para-Benziporphyrins: Synthesis and Aromaticity Switching. *Chem. - A Eur. J.* **2014**, *20* (7), 1985–1997.

(26) Stępień, M.; Latos-Grazyński, L. Tetraphenyl-p-Benziporphyrin: A Carbaporphyrinoid with Two Linked Carbon Atoms in the Coordination Core. *J. Am. Chem. Soc.* **2002**, *124* (15), 3838–3839.

(27) Jeong, S. D.; Sessler, J. L.; Lynch, V.; Lee, C. H. Dithiabenzisapphyrin: A Core-Modified Sapphyrin Bearing Exocyclic Double Bonds at the Meso-Positions. *J. Am. Chem. Soc.* **2008**, *130* (2), 390–391.

(28) Srinivasan, A.; Pushpan, S. K.; Kumar, M. R.; Mahajan, S.; Chandrashekar, T. K.; Roy, R.; Ramamurthy, P. Meso-Aryl Sapphyrins with Heteroatoms; Synthesis, Characterization, Spectral and Electrochemical Properties. *J. Chem. Soc. Perkin Trans. 2* **1999**, *0* (5), 961–968.

(29) Srinivasan, A.; Reddy, V. R. M.; Jeyaprakash Narayanan, S.; Sridevi, B.; Pushpan, S. K.; Ravikumar, M.; Chandrashekar, T. K. Tetrathia- and Tetraoxarubyrins: Aromatic, Core-Modified, Expanded Porphyrins. *Angew. Chem. Int. Ed.* **1997**, *36* (23), 2598–2601.

(30) Ghosh, A.; Maity, D. K.; Ravikanth, M. Aluminium(III) Porphyrin Based Axial-Bonding Type Dyads Containing Thiaporphyrins and Expanded Thiaporphyrins as

Axial Ligands. *New J. Chem.* **2012**, *36* (12), 2630–2641.

(31) Higashino, T.; Lim, J. M.; Miura, T.; Saito, S.; Shin, J. Y.; Kim, D.; Osuka, A. Möbius Antiaromatic Bisphosphorus Complexes of [30]Hexaphyrins. *Angew. Chem. Int. Ed.* **2010**, *49* (29), 4950–4954.

(32) Osuka, A.; Saito, S. Expanded Porphyrins and Aromaticity. *Chem. Commun.* **2011**, *47* (15), 4330–4339.

(33) Geuenich, D.; Hess, K.; Köhler, F.; Herges, R. Anisotropy of the Induced Current Density (ACID), a General Method to Quantify and Visualize Electronic Delocalization. *Chem. Rev.* **2005**, *105* (10), 3758–3772.

(34) Stępień, M.; Latos-Grażyński, L. Tetraphenylbenziporphyrin—A Ligand for Organometallic Chemistry. *Chem. - A Eur. J.* **2001**, *7* (23), 5113–5117.

(35) Lash, T. D.; Toney, A. M.; Castans, K. M.; Ferrence, G. M. Synthesis of Benziporphyrins and Heterobenziporphyrins and an Assessment of the Diatropic Characteristics of the Protonated Species. *J. Org. Chem.* **2013**, *78* (18), 9143–9152.

(36) Xu, X. L.; Li, Z. Catalytic Electrophilic Alkylation of P-Quinones through a Redox Chain Reaction. *Angew. Chem. Int. Ed.* **2017**, *56* (28), 8196–8200.

(37) Lash, T. D.; Szymanski, J. T.; Ferrence, G. M. Tetraaryldimethoxybenziporphyrins. At the Edge of Carbaporphyrinoid Aromaticity. *J. Org. Chem.* **2007**, *72* (17), 6481–6492.

(38) Frisch, M. J.; Trucks, G. W.; Schlegel, H. B.; Scuseria, G. E.; Robb, M. A.; Cheeseman, J. R.; Scalmani, G.; Barone, V.; Mennucci, B.; Petersson, G. A.; et al. *Gaussian 09 C.01*; Gaussian Inc.: Wallingford CT, 2009.

(39) Treutler, O.; Ahlrichs, R. Efficient Molecular Numerical Integration Schemes. *J. Chem. Phys.* **1995**, *102* (1), 346–354.

(40) Becke, A. D. A New Mixing of Hartree–Fock and Local Density-Functional Theories. *J. Chem. Phys.* **1993**, *98* (2), 1372–1377.

(41) Hehre, W. J. Ab Initio Molecular Orbital Theory. *Acc. Chem. Res.* **1976**, *9* (11), 399–406.

(42) Bauernschmitt, R.; Ahlrichs, R. Treatment of Electronic Excitations within the Adiabatic Approximation of Time Dependent Density Functional Theory. *Chem. Phys. Lett.* **1996**, *256* (4–5), 454–464.

(43) Furche, F.; Rappoport, D. *Computational Photochemistry (Google EBook)*; Olivucci, M., Ed.; Elsevier: Amsterdam, 2005.

(44) Gabe, Y.; Ueno, T.; Urano, Y.; Kojima, H.; Nagano, T. Tunable Design Strategy for Fluorescence Probes Based on 4-Substituted BODIPY Chromophore: Improvement of Highly Sensitive Fluorescence Probe for Nitric Oxide. *Anal. Bioanal. Chem.* **2006**, *386* (3), 621–626.

(45) Furche, F.; Ahlrichs, R. Adiabatic Time-Dependent Density Functional Methods for Excited State Properties. *J. Chem. Phys.* **2002**, *117* (16), 7433–7447.

(46) *Practical Aspects of Computational Chemistry: Methods, Concepts and Applications (Google EBook)*; Leszczynski, J., Shukla, M., Eds.; Springer, 2009.

(47) Scalmani, G.; Frisch, M. J.; Mennucci, B.; Tomasi, J.; Cammi, R.; Barone, V. Geometries and Properties of Excited States in the Gas Phase and in Solution: Theory and Application of a Time-Dependent Density Functional Theory Polarizable Continuum Model. *J. Chem. Phys.* **2006**, *124* (9), 94107–94115.

(48) Thorat, K. G.; Kamble, P.; Mallah, R.; Ray, A. K.; Sekar, N. Congeners of Pyrromethene-567 Dye: Perspectives from Synthesis, Photophysics, Photostability, Laser, and TD-DFT Theory. *J. Org. Chem.* **2015**, *80* (12).

(49) Thorat, K. G.; Kamble, P. S.; Ray, A. K.; Sekar, N. Novel Pyrromethene Dyes with N-Ethyl Carbazole at Meso Position: Comprehensive Photophysical, Lasing, Photostability and TD-DFT Study. *Phys. Chem. Chem. Phys.* **2015**, *17*, 17221–17236.

(50) Cossi, M.; Barone, V.; Cammi, R.; Tomasi, J. Ab Initio Study of Solvated Molecules: A New Implementation of the Polarizable Continuum Model. *Chem. Phys. Lett.* **1996**, *255* (4–6), 327–335.

(51) Tomasi, J.; Mennucci, B.; Cammi, R. Quantum Mechanical Continuum Solvation Models. *Chem. Rev.* **2005**, *105* (8), 2999–3093.

Table of Contents